AIMS Biophysics, 8(2): 221–232.
DOI: 10.3934/biophy.2021016
Received: 22 March 2021
Accepted: 06 May 2021
Published: 08 May 2021

http://www.aimspress.com/journal/biophysics

Research article

Double energy profile of pBR322 plasmid

Ludmila V. Yakushevich[1,*] and Larisa A. Krasnobaeva[2,3]

[1] Institute of Cell Biophysics, Russian Academy of Sciences, 142290 Pushchino. Institutskaya str. 3, Moscow region, Russia
[2] Siberian State Medical University, 634050 Tomsk, Moscow tract 2, Russia
[3] Tomsk State University, 634050 Tomsk, Lenin Avenue 36, Russia

*** Correspondence:** Email: kind-@mail.ru; Tel: +74967730252; Fax: +74967330509.

Abstract: A small circular DNA - plasmid pBR322, is considered as a complex dynamic system where nonlinear conformational perturbations which are often named open states or kinks, can arise and propagate. To describe the internal dynamics of the plasmid we use mathematical model consisting of two coupled sine-Gordon equations that in the average field approximation are transformed to two sine-Gordon independent equations with renormalized coefficients. The first equation describes angular oscillations of nitrous bases of the main chain. The second equation describes angular oscillations of nitrous bases in the complementary chain. As a result, two types of kink-like solutions have been obtained. One type kinks were the solutions of the first equation, and the other kinks were the solutions of the second equation. We calculated the main characteristics of the kink motion, including the time dependences of the kink velocity, coordinates, and total energy. These calculations were performed at the initial velocity equal to 1881 m/s which was chosen to avoid reflections from energy barriers corresponding to CDS-1 and CDS-2. The movement of the kinks was investigated by the method of the double energy profile. The maximum complete set of the DNA dynamic parameters was used to calculate the double profile. To calculate the velocity, energy and trajectory of the kinks, the block method was used. The results obtained made it possible to explain in which region of the plasmid the formation of a transcription bubble is most likely, as well to understand in which direction the bubble will move and the transcription process will go.

Keywords: plasmid pBR322; double profile; open states; kinks; transcription bubbles; direction of transcription

1. Introduction

The construction of energy profiles and their analysis is a new method for studying the physical and functional properties of plasmids. This method came to DNA science from theoretical physics and nonlinear mathematics. In the frameworks of the method, the DNA molecule is considered as a complex dynamic system in which nonlinear conformational perturbations-kinks, can arise and propagate [1–4].

Since the work [5], kinks have been actively used to simulate the DNA open states which are small (only a few base pairs long) unwound DNA regions inside which hydrogen bonds between complementary bases are broken. The behavior of the kinks is in many ways similar to that of ordinary particles moving in the DNA potential field. Having calculated the energy profile of the potential field, one can completely solve the problem of the kink dynamics including calculation of time dependence of the kink velocity and construction of the kink trajectory.

A particular example of the open state is the transcription bubble (Figure 1) which is formed at the initial stage of the transcription process as a result of the interaction of RNA polymerase with DNA promoter region [6,7]. One of the first attempts to calculate the DNA potential field in which the transcriptional bubble moves was made by Salerno [8]. However, the absence at that time of a complete set of dynamic parameters of DNA, as well as the computer power required for such calculations, forced the author to confine himself to only a small fragment of a DNA molecule, which did not allow to obtain reliable results on the kink dynamics and to relate them with functional properties of the molecule.

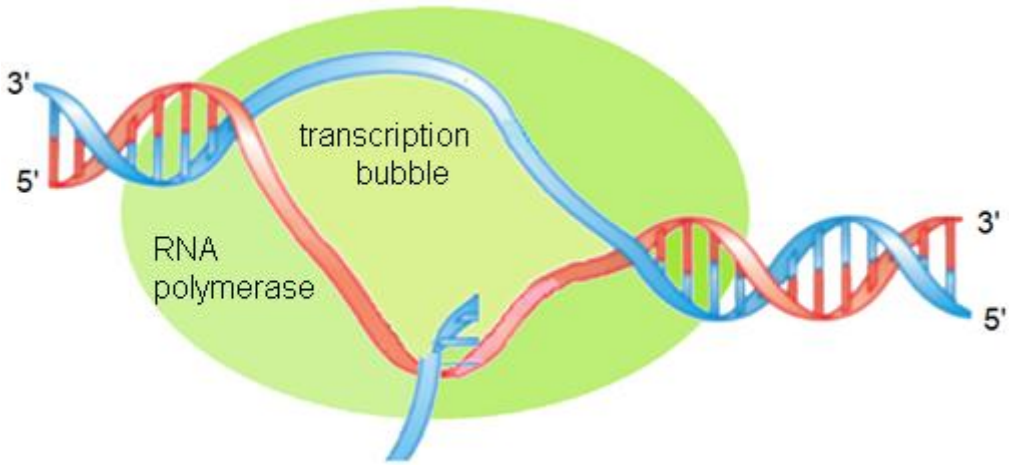

Figure 1. Transcription bubble.

In this work, we solve this problem on the basis of new data and new approaches to the study of the dynamics of open states in inhomogeneous DNA. In the calculations we use the full set of dynamic parameters of DNA, which was first obtained in [9] and later refined in [10]. The block method and the method of constructing the kinks trajectories are also applied [11,12]. In contrast to work [12], where only one plasmid profile was calculated, here we use the method of the double profile, which makes it possible to compare the dynamic characteristics of kinks activated in the main and complementary DNA strands. Such a comparison makes it possible to explain in which

region of the plasmid the formation of a transcription bubble is most likely, as well to understand in which direction the bubble will move and the transcription process will go.

2. Structure of plasmid pBR322

Plasmid pBR322 [13] is a small circular DNA the sequence of which consists of 4361 bases [14] (Appendix). This sequence contains three coding regions:

CDS-1, encoding tetracycline resistance protein,
CDS-2, encoding ROP protein,
CDS-3, encoding beta-lactamase,

and three promoters: P1, P2 and P3 marked in Appendix by grey. Coordinates of the CDS regions are (86..1276), (1915..2106) and (3293..4153). Coordinates of promoters are (27-33), (43-49) and (4188-4194). The double-stranded scheme of the plasmid is shown in Figure 2a. A linear version of the scheme obtained by cutting at the point Q, is presented in Figure 2b.

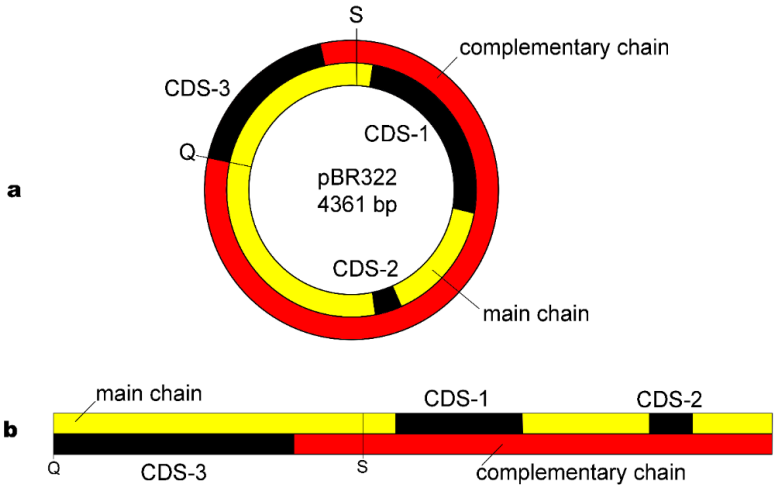

Figure 2. Double-stranded scheme of the pBR32 plasmid (a) and its linear analogue (b). Q is the cutting point. S is the starting point. CDS-1, CDS-2 and CDS-3 are coding regions.

Table 1. Details of the structure of the main/complementary sequences of the pBR32 plasmid.

Region number	Region coordinates	N_A	N_T	N_G	N_C	N
1	1..85	22/29	29/22	17/17	17/17	85
2 (CDS-1)	86..1276	190/268	268/190	353/381	381/353	1192
3	1277..1914	142/145	145/142	160/191	191/160	638
4 (CDS-2)	1915..2106	54/37	37/54	48/53	53/48	192
5	2107..3292	294/268	268/294	319/305	305/319	1186
6 (CDS-3)	3293..4153	213/223	223/213	203/222	222/203	861
7	4154-4361	67/64	64/67	34/42	42/34	207

It is convenient to renumber all regions including CDS regions and the regions between them,

starting from the point S. A total of 7 regions turned out. Data on their composition are presented in Table 1.

However, the splitting of the sequence into 7 regions does not reflect the circular nature of the plasmid. To take this into account, we combined the 1st and 7th regions into a single region with number (7 + 1). As a result, the total number of regions decreased by one and became equal to six. In what follows, these six regions will be referred to as blocks.

3 Model and methods

To describe angular oscillations of nitrous bases in a separate block of the DNA molecule consisting of N bp, let us use the improved Englander model [5], which is a system of 2N coupled nonlinear differential equations [15]:

$$\begin{aligned} &I_{\mathrm{n},1}\frac{d^2\varphi_{n,1}(t)}{dt^2} - K'_{n,1}\left[\varphi_{n+1,1}(t) - 2\varphi_{n,1}(t) + \varphi_{n-1,1}(t)\right] + \\ &+k_{n,1-2}R_{\mathrm{n},1}(R_{\mathrm{n},1} + R_{n,2})\ \sin\varphi_{n,1} - k_{n,1-2}R_{\mathrm{n},1}R_{\mathrm{n},2}\sin(\varphi_{n,1} - \varphi_{n,2}) = \\ &= -\beta_{n,1}\frac{d\varphi_{n,1}(t)}{dt}, \end{aligned} \tag{1}$$

$$\begin{aligned} &I_{n,2}\frac{d^2\varphi_{n,2}(t)}{dt^2} - K'_{n,2}\left[\varphi_{n+1,2}(t) - 2\varphi_{n,2}(t) + \varphi_{n-1,2}(t)\right] + \\ &+k_{n,1-2}R_{\mathrm{n},2}(R_{\mathrm{n},1} + R_{\mathrm{n},2})\sin\varphi_{n,2} - k_{\mathrm{n},1\text{-}2}R_{\mathrm{n},1}R_{\mathrm{n},2}\sin(\varphi_{n,2} - \varphi_{n,1}) = \\ &= -\beta_{n,2}\frac{d\varphi_{n,2}(t)}{dt}. \end{aligned} \tag{2}$$

Here $\varphi_{n,i}(t)$ is the angular deviation of the *n*-th nitrous base of the *i*-th chain; $I_{n,i}$ is the moment of inertia of the *n*-th nitrous base of the *i*-th chain; $R_{n,i}$ is the distance between the center of mass of the *n*-th nitrous base of the *i*-th chain and the sugar-phosphate backbone; $K'_{n,1} = KR^2_{n,i}$; *K* is the rigidity (in tension) of the sugar-phosphate backbone; $\beta_{n,i} = \alpha R^2_{n,i}$, α is the dissipation coefficient; $k_{n,i}$ is a constant characterizing the interaction between bases within pairs; *i* = 1, 2; *n* = 1, 2, ... *N*.

Equations (1)-(2) are simplified if we use the concentration method where the coefficients $I_{n,i}$, $R_{n,i}$, $K'_{n,i}$, $k_{n,1\text{-}2}$ and $\beta_{n,i}$ are averaged according to the following formulas [16]:

$$\begin{aligned} &I_{n,i} \to \bar{I}_i = I_A C_{A,i} + I_T C_{T,i} + I_G C_{G,i} + I_C C_{C,i}, \\ &R_{n,i} \to \bar{R}_i = R_A C_{A,i} + R_T C_{T,i} + R_G C_{G,i} + R_C C_{C,i}, \\ &K'_{n,i} \to \bar{K}'_i = K'_A C_{A,i} + K'_{\mathrm{T}} C_{T,i} + K'_{\mathrm{G}} C_{G,i} + K'_{\mathrm{C}} C_{C,i}, \\ &k_{n,1\text{-}2} \to \bar{k}_{1-2} = k_{A-T}\left(C_{A,1} + C_{T,2}\right) + k_{G-C}\left(C_{G,1} + C_{C,2}\right), \\ &\beta_{n,i} \to \bar{\beta}_i = \beta_{\mathrm{A}} C_{A,i} + \beta_T C_{T,i} + \beta_G C_{G,i} + \beta_C C_{C,i}. \end{aligned} \tag{3}$$

where $C_{j.i} = N_{j,i}/N$ is the concentration of bases of the *j*-th type in the *i*-th chain; $N_{j,i}$ is the number of the of bases *j*-th type in the *i*-th sequence; (*j* = A, T, G, C); (*i* = 1, 2).

After the averaging procedure (3), equations (1)–(2) are transformed to the form:

$$\begin{aligned}&\bar{I}_1\frac{d^2\varphi_{n,1}(t)}{dt^2}-\bar{K}_1'[\varphi_{n+1,1}(t)-2\varphi_{n,1}(t)+\varphi_{n-1,1}(t)]+\\&+\bar{k}_{1-2}\bar{R}_1(\bar{R}_1+\bar{R}_2)\ \sin\varphi_{n,1}-\bar{k}_{1-2}\bar{R}_1\bar{R}_2\sin(\varphi_{n,1}-\varphi_{n,2})=\\&=-\bar{\beta}_1\frac{d\varphi_{n,1}(t)}{dt},\end{aligned}\tag{4}$$

$$\begin{aligned}&\bar{I}_2\frac{d^2\varphi_{n,2}(t)}{dt^2}-\bar{K}_2'[\varphi_{n+1,2}(t)-2\varphi_{n,2}(t)+\varphi_{n-1,2}(t)]+\\&+\bar{k}_{1-2}\bar{R}_2(\bar{R}_1+\bar{R}_2)\ \sin\varphi_{n,2}-\bar{k}_{1-2}\bar{R}_1\bar{R}_2\sin(\varphi_{n,2}-\varphi_{n,1})=\\&=-\bar{\beta}_2\frac{d\varphi_{n,2}(t)}{dt}.\end{aligned}\tag{5}$$

In the continuum approximation, these equations take the following form:

$$\begin{aligned}&\bar{I}_1\varphi_{1tt}-\bar{K}_1'a^2\varphi_{1zz}+\bar{k}_{1-2}\bar{R}_1(\bar{R}_1+\bar{R}_2)\ \sin\varphi_1-\bar{k}_{1-2}\bar{R}_1\bar{R}_2\sin(\varphi_1-\varphi_2)=\\&=-\bar{\beta}_1\varphi_{1t},\end{aligned}\tag{6}$$

$$\begin{aligned}&\bar{I}_2\varphi_{2tt}-\bar{K}_2'a^2\varphi_{2zz}+\bar{k}_{1-2}\bar{R}_1(\bar{R}_1+\bar{R}_2)\ \sin\varphi_2-\bar{k}_{1-2}\bar{R}_1\bar{R}_2\sin(\varphi_2-\varphi_1)=\\&=-\bar{\beta}_2\varphi_{2t}.\end{aligned}\tag{7}$$

In the approximation of average field [17], two coupled equations (6) and (7) are transformed into two independent equations:

$$\bar{I}_1\varphi_{1tt}-\bar{K}_1'a^2\varphi_{1zz}+\bar{k}_{1-2}\bar{R}_1^2\sin\varphi_1=-\bar{\beta}_1\varphi_{1t},\tag{8}$$

$$\bar{I}_2\varphi_{2tt}-\bar{K}_2'a^2\varphi_{2zz}+\bar{k}_{1-2}\bar{R}_2^2\sin\varphi_1=-\bar{\beta}_2\varphi_{2t},\tag{9}$$

where *a* is the distance between the nearest base pairs. In this approximation, the movement of kinks in the main and complementary chains can be considered separately. The validity of this approximation for DNA was shown in [18], where it was demonstrated numerically that taking into account the interaction between kinks activated in the main and complementary chains leads only to a slight perturbation of the kink shape.

One-soliton solutions of equations (8)–(9), kinks, have then the form :

$$\begin{aligned}\varphi_{k,1}(z,t)&=4\,\mathrm{arctg}\{\exp[(\gamma_{k,1}/d_{k,1})(z-\upsilon_{k,1}(t)t-z_{0,1})]\},\\\varphi_{k,2}(z,t)&=4\,\mathrm{arctg}\{\exp[(\gamma_{k,2}/d_{k,2})(z-\upsilon_{k,2}(t)t-z_{0,2})]\}.\end{aligned}\tag{10}$$

Here $\upsilon_{k,i}(t)$ is the time dependent kink velocity, $\gamma_{k,i}(t)=(1-\upsilon_{k,i}^2(t)/\bar{C}_i^2)^{-\frac{1}{2}}$ is the Lorentz factor, $\bar{C}_i=(\bar{K}_i'a^2/\bar{I}_i)^{1/2}$ is the sound velocity in the *i*-th chain, $d_{k,i}=(\bar{K}_i'a^2/\bar{V}_i)^{1/2}$ is the size of the kink in the *i*-th chain, $\bar{V}_i=\bar{k}_{1-2}\bar{R}_i^2$.

Equation for the kink velocity was obtained by McLaughlin and Scott [19]. In the case of plasmid pBR322, this equation has the form:

$$\frac{d\upsilon_{k,i}(t)}{dt}=-\frac{\bar{\beta}_i}{\bar{I}_i}\upsilon_{k,i}(t)\left[1-\left(\frac{\upsilon_{k,i}(t)}{\bar{C}_i}\right)^2\right],\qquad(i=1,2)\tag{11}$$

The analytical solution of equation (1) found in [20], has the form :

$$\upsilon_{k,i}(t) = \frac{\upsilon_{0,i}\bar{\gamma}_{0,i}\exp\left(-\frac{\bar{\beta}_i}{\bar{I}_i}(t-t_0)\right)}{\sqrt{1+\left(\frac{\upsilon_{0,i}\bar{\gamma}_{0,i}}{\bar{C}_i}\right)^2\exp\left(-\frac{2\bar{\beta}_i}{\bar{I}_i}(t-t_0)\right)}} \tag{12}$$

where $\upsilon_{0,i}$ is the kink velocity at the initial moment of time t_0, $\bar{\gamma}_{0,i} = (1-\upsilon_{0,i}^2/\bar{C}_i^2)^{-1/2}$.

The solution for the kink coordinate $z_{k,i}(t)$ determined by the relation $\upsilon_{k,i}(t) = \frac{dz_{k,i}(t)}{dt}$, was obtained in [12]:

$$z_{k,i} = z_0 - \bar{C}_i\frac{\bar{I}_i}{\bar{\beta}_i}\arcsin\left(\frac{\upsilon_{0,i}}{\bar{C}_i}\bar{\gamma}_{0,i}\exp\left(-\frac{\bar{\beta}_i}{\bar{I}_i}(t-t_0)\right)\right) + \bar{C}_i\frac{\bar{I}_i}{\bar{\beta}_i}\arcsin\left(\frac{\upsilon_{0,i}}{\bar{C}_i}\bar{\gamma}_{0,i}\right) \tag{13}$$

where z_0 is the coordinate of the kink at the initial moment of time t_0.

The total kink energy is determined by the following formula [21]:

$$E_i = \frac{\boldsymbol{E_{0,i}}}{\sqrt{1-\frac{\upsilon_{k,i}^2}{\bar{C}_i^2}}}, \tag{14}$$

where $E_{0,i}$ is the rest energy (or the energy of activation) of the kink:

$$E_{0,i} = 8\sqrt{\bar{K}_i'\bar{V}_i} \quad (i = 1, 2). \tag{15}$$

In the case of small velocities ($\upsilon_{k,i} \ll \mathrm{C}_i$), formula (11) takes the form:

$$E_i = \frac{E_{0,i}}{\sqrt{1-\frac{\upsilon_{k,i}^2}{\bar{C}_i^2}}} = E_{0,i} + \frac{m_{k,i}\upsilon_{k,i}^2}{2}, \tag{16}$$

where ($m_{k,i} = \frac{E_{0,i}}{2\bar{C}_i^2}$) is the mass of the kink in the *i*-th chain. Formula (13) confirms that kink can be modeled as a quasiparticle with mass $m_{k,i}$, velocity $\upsilon_{k,i}$ and potential energy $E_{0,i}$.

4. Results and discussion

4.1. Energy profile of the main and complementary plasmid sequences

To construct the energy profile, we first calculated the averaged values of the main dynamic parameters of the plasmid: $\tilde{I}^{(i)}$, $\tilde{K}'^{(i)}$, $\tilde{V}^{(i)}$, for each of the six regions:

$$\tilde{I}^{(i)} = I_A C_A^{(i)} + I_T C_T^{(i)} + I_G C_G^{(i)} + I_C C_C^{(i)},$$

$$\tilde{K}'^{(i)} = K'_A C_A^{(i)} + K'_T C_T^{(i)} + K'_G C_G^{(i)} + K'_C C_C^{(i)} \tag{17}$$

$$\tilde{V}^{(i)} = V_A C_A^{(i)} + V_T C_T^{(i)} + V_G C_G^{(i)} + V_C C_C^{(i)},$$

and also calculated the values of the rest energies of the kinks activated in each of these regions:

$$\tilde{E}_0^{(i)} = 8\sqrt{\tilde{K}'^{(i)}\tilde{V}^{(i)}}. \quad (18)$$

Here $\tilde{I}^{(i)}$ is the averaged moment of inertia of the nitrous bases of the *i*-th region; $\tilde{K}'^{(i)}$ is the torsion rigidity in the *i*-th region; $\tilde{V}^{(i)}$ is a constant characterizing the interaction between complementary bases in the *i*-th region, $i = 1, 2,\ldots 6$. The calculation results are presented in Table 2.

Table 2. Dynamic characteristics calculated for each of the six regions of the main/complementary sequences of the pBR32 plasmid.

Number of the region	Coordinate of the region	$\tilde{I}^{(i)} \times 10^{-44}$ (kg·m^2)	$\tilde{K}'^{(i)} \times 10^{-18}$ (N·m)	$\tilde{V}^{(i)} \times 10^{-20}$ (J)	$\tilde{E}_0^{(i)} \times 10^{-18}$ (J)
1+7	(1..85)+(4154..4361)	6.13/6.28	1.94/1.97	2.06/2.10	1.60/1.63
2 (CDS-1)	86..1276	6.05/6.33	1.90/1.97	2.26/2.32	1.66/1.71
3	1277..1914	6.09/6.30	1.92/1.96	2.21/2.26	1.65/1.68
4 **(**CDS-2)	1915..2106	6.26/6.13	1.97/1.92	2.23/2.19	1.67/1.64
5	2107..3292	6.25/6.14	1.95/1.93	2.22/2.20	1.67/1.65
6 (CDS-3)	3293..4153	6.14/6.25	1.93/1.95	2.17/2.20	1.64/1.66

With the help of the data from the last column of Table 2 we constructed the double energy profile of the potential field of the plasmid (Figure 3). The energy was calculated not at every point, but for each range into which we divided the plasmid. The coordinates of the bases are plotted in Figure 3 along the horizontal in units of base pairs (bp), 1 bp = 3.4×10^{-10} m. The values of the rest energy of kinks are plotted along the vertical.

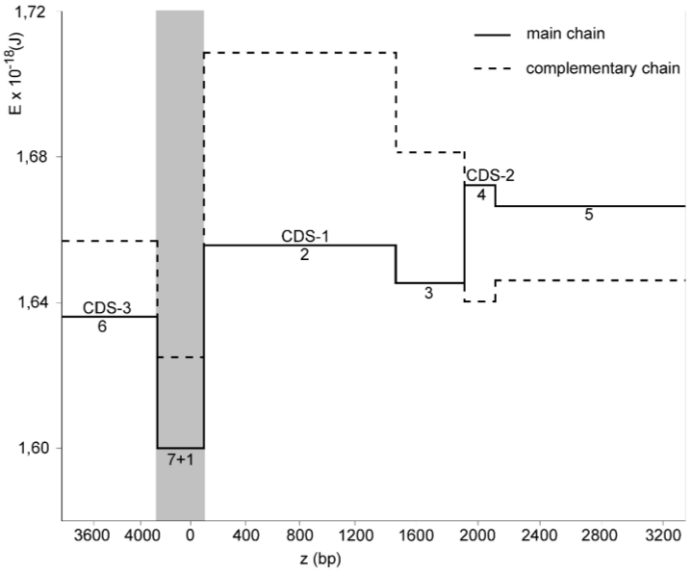

Figure 3. Double energy profile of the pBR32 plasmid. Solid line corresponds to the main sequence and the dashed line corresponds to complementary sequence. Grey band indicates (7 + 1)-th range.

Figure 3 shows that the deepest well in the energy profile of both the main (solid line) and complementary (dashed line) sequences corresponds to the (7 + 1)-th region. This means that the probability of kink activation in this region is the highest. This result is in good agreement with the experimental data summarized in [14]. Indeed. the transcription process usually begins with the binding of RNA polymerase to the promoter region of the DNA sequence, and this event is accompanied by local unwinding double-stranded DNA. According to [14] there are three promoters in the (7 + 1)-th region: the P2 promoter located in the main chain, and the P1 and P3 promoters located in the complementary chain. That saturation of the (7 + 1)-th region with promoters indicates that just in this region with high probability the formation of local unwound regions - kinks, takes place.

It can be seen also that in the (7 + 1)-th region, the rest energy of the kinks activated in the main strand is less than the rest energy of the kinks activated in the complementary strand. This means that the probability of the kink activation in the main strand containing P2 promoter is greater than in the complementary strand containing P1 and P3 promoters. This allows us to suggest that the P1 and P3 promoters are much weaker than the P2 promoter.

4.2. Velocity, coordinate, energy and trajectories of kinks in plasmid pBR322

Using formulas (2)-(4) and the data of Table 2, we plotted the time dependence of the velocity, coordinates and total energy of the plasmid pBR322 kinks (Figures 4–6).

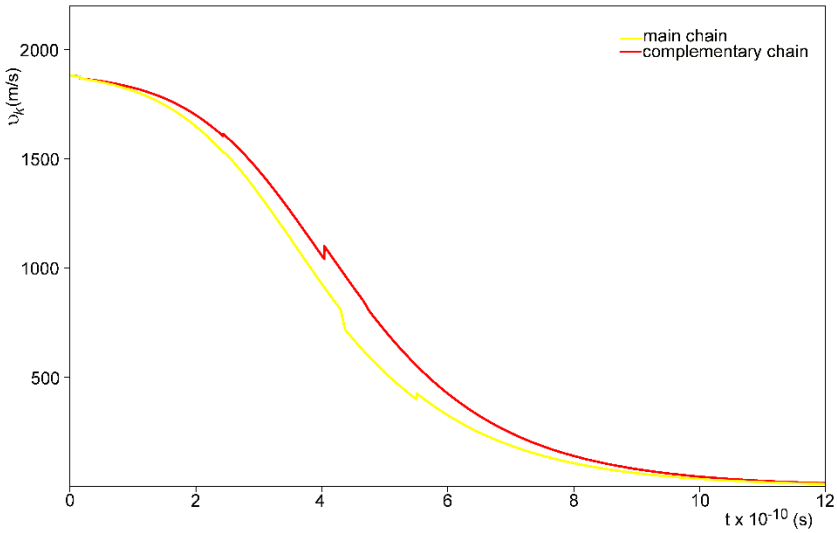

Figure 4. Time dependence of the velocity of kinks activated in the main and complementary sequences of plasmid pBR322. The initial velocity of the kink is 1881 m/s. The dissipation coefficient is 0.126×10^{-14} J·s/m^2.

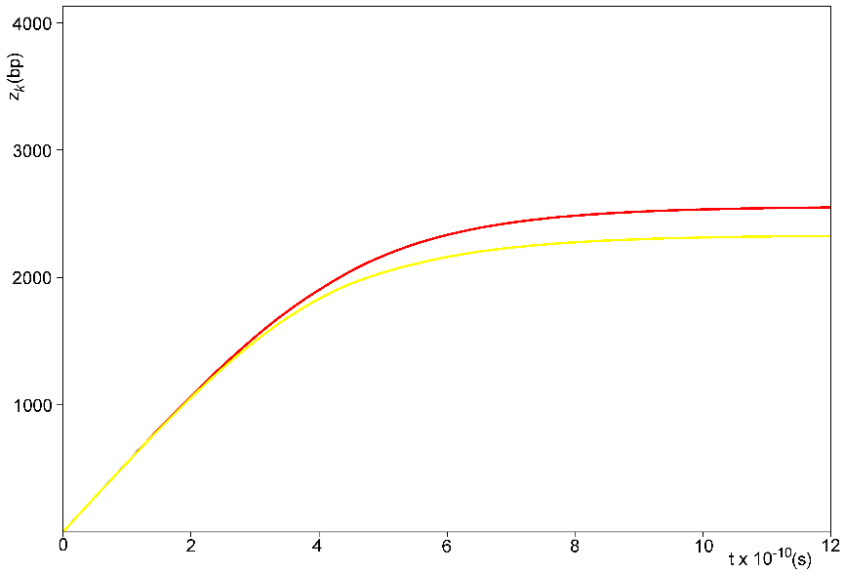

Figure 5. Time dependence of the coordinates of kinks activated in the main and complementary sequences of plasmid pBR322. The yellow line corresponds to the main sequence and the red line corresponds to the complementary sequence. The initial velocity of the kink is 1881 m/s. The dissipation coefficient is 0.126×10^{-14} J·s/m^2.

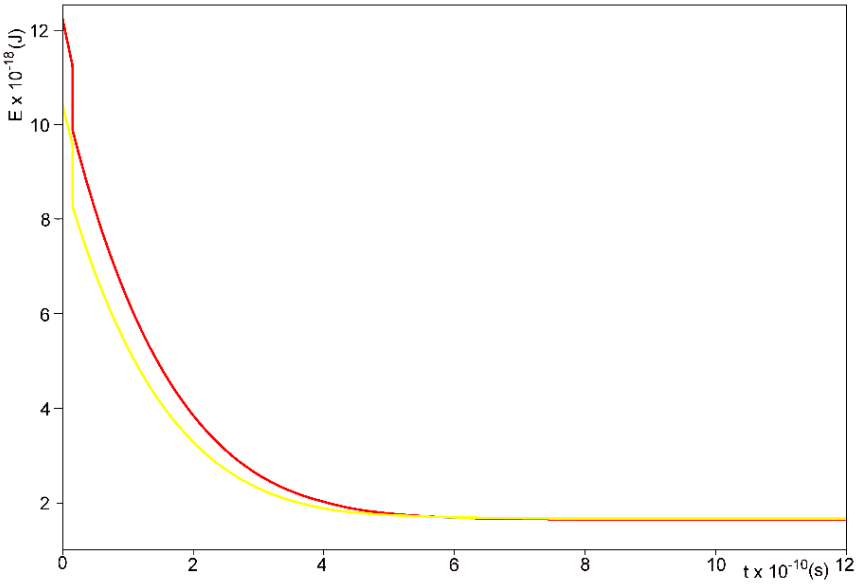

Figure 6. Time dependence of the total energy of kinks activated in the main and complementary sequences of plasmid pBR322. The yellow line corresponds to the main sequence and the red line corresponds to the complementary sequence. The initial velocity of the kink is 1881 m/s. The dissipation coefficient is 0.126×10^{-14} J·s/m^2.

Figure 4 shows that the velocity of the kinks activated in both strands decreases with time, which is explained by the effects of dissipation. The velocity of the kink activated in the complementary

strand, decreases faster. The zigzags observed on both curves are explained by abrupt changes in the velocity of the kinks when passing the boundaries between the regions.

Figure 5 shows that the coordinate of the kinks grows smoothly and reaches a constant value, which means that the kink movement stops. Kink activated in the main strand stops at the point 2332 bp, and kink activated in the complementary strand stops at 2558 bp.

From Figure 6 it can be seen that at the same value of the initial kink velocity (1881 m/s), the values of the initial total energy of the kinks activated in different strands differ. For kinks activated in the main strand, the initial total energy is 10.42×10^{-18} (J), and for kinks activated in the complementary strand, the initial total energy is 12.25×10^{-18} (J). Later both energy curves decreases and reaches the values of the rest energies.

To construct trajectories of kinks in the 3D space, we solved numerically a system of coupled differential equations for the velocity and coordinates of the kinks:

$$\frac{d\tilde{z}_k^{(i)}(t)}{dt} = \tilde{v}_k^{(i)}(t), \tag{19}$$

$$\frac{d\tilde{v}_k^{(i)}(t)}{dt} = -\frac{\tilde{\beta}^{(i)}}{\tilde{I}^{(i)}}\tilde{v}_k^{(i)}(t)\left[1 - \left(\frac{\tilde{v}_k^{(i)}(t)}{\tilde{C}^{(i)}}\right)^2\right]. \; i = 1,2,\ldots 6 \tag{20}$$

The results are presented in the form of trajectories of the kink motion in the space {v, z, t} (Figure 7).

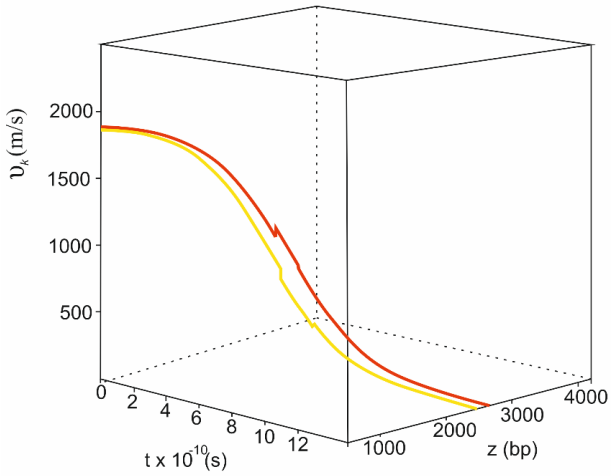

Figure 7. Trajectories of the pBR322 kinks in the 3D space. The yellow line corresponds to the main sequence and the red line corresponds to the complementary sequence. The initial velocity of the kink is 1881 m/s. The dissipation coefficient is 0.126×10^{-14} J·s/m^2.

5. Conclusions

In the present work, we investigated the dynamics of the nonlinear conformation distortions – kinks, activated in the plasmid pBR322. The kinks were considered as quasi particles moving in the potential field of the plasmid. The key moment of the method used is the construction of the double energetic profile the analysis of which gives valuable information about the kink behavior.

To imitate the internal dynamics of the plasmid we used mathematical model consisting of two coupled sine-Gordon equations that in the average field approximation were transformed to two sine-Gordon independent equations with renormalized coefficients. The first equation described angular oscillations of nitrous bases of the main chain in the complementary chain. The second equation described angular oscillations of nitrous bases in the complementary chain. As a result, we obtained two types of kink-like solutions: one type are kinks which were the solutions of the first equation, and the other are kinks which were the solutions of the second equation.

To take into account the circular nature of DNA, we combined the end regions into a single block. Using calculated values of the rest energies of the kinks we constructed two energy profiles: the first for the main sequence, the second for the complementary one.

Analysis of these profiles showed that the deepest well in the energy profiles corresponds to the (7 + 1)-th region. This means that the probability of kink activation in this region is the highest.

Because the kink rest energy in the (7 + 1)-th region of the main sequence is less than in that of the complementary sequence we concluded that the P2 promoter located in the (7 + 1)-th region of the main sequence is stronger than the P1 and P3 promoters located in the (7 + 1)-th region of the complementary sequence. Therefore, it can be assumed that the transcription bubble formed in the (7 + 1)-th region is most likely to start moving in the direction of the CDS-1 region.

We calculated the main characteristics of the kink motion, including the time dependences of the kink velocity, coordinates, and total energy. These calculations were performed at the initial velocity equal to 1881 m/s which was chosen to avoid reflections from energy barriers corresponding to CDS-1 and CDS-2. Despite the fact that here we have considered only one value of the initial kink velocity the proposed approach is applicable to any values of the initial kink velocity. It is necessary only to keep in mind one important condition: the initial values should be less than the sound velocity. This condition arises from the mathematical requirements for the existence and stability of the solution in the form of kink.

It should be noted, also, that these results were obtained under three additional constraints. First, we used a simplified model that took into account angular oscillations of the nitrous bases in only one of the two DNA strands. Second, only one type of internal DNA motions-angular oscillations of the nitrous bases, was taken into accountю. Third, the model used did not take into account the DNA torque. In spite of all these limitations, we can expect that the results of the investigations obtained by simple and convenient method correctly convey the basic laws of the kink dynamic behavior in plasmid pBR322 and can be applied to another DNA sequences.

Conflict of interest

All authors declare no conflicts of interest in this paper.

References

1. Yakushevich LV (2006) *Nonlinear physics of DNA*, Weinheim: Wiley.
2. Dauxois T, Peyrard M (2006) *Physics of Solitons*, Cambridge: Cambridge University Press.
3. Shapovalov AV, Krasnobaeva LA (2009) *Solitons of the sine-Gordon equation*. Tomsk: TGU. Available from: http://vital.lib.tsu.ru/vital/access/manager/Repository/vtls:000392302.

4. Ivancevic VG, Ivancevic TT (2013) Sine-Gordon solitons, kinks and breathers as physical models of nonlinear excitations in living cellular structures. *J Geom Symmetry Phys* 31: 1–56.
5. Englander SW, Kallenbach NR, Heeger AJ, et al (1980) Nature of the open state in long polynucleotide double helices: possibility of soliton excitations. *Proc Natl Acad Sci USA* 77: 7222–7226.
6. Forth S, Sheinin MY, Inman J, et al. (2013) Torque measurement at the single-molecule level. *Annu Rev Biophys* 42: 583–604.
7. Severin ES (ed) (2020) *Biochemistry*. Moscow: GEOTAR–Media. Available from: https://expose.gpntbsib.ru/expose/vnp-4f32781c/book/E2019-3257830172062.
8. Salerno M (1995) Nonlinear dynamics of plasmid *pBR*322 promoters. In: Peyrard M (ed) *Nonlinear Excitations in Biomolecules*. New York: Springer, 147–153.
9. Yakushevich LV, Krasnobaeva LA, Shapovalov AV, et al. (2005) One-and two-soliton solutions of the sine-Gordon equation as applied to DNA. *Biophysics* 50: 450–455.
10. Yakushevich LV, Krasnobaeva LA (2016) Forced oscillations of DNA bases. *Biophysics* 61: 241–250.
11. Grinevich AA, Ryasik AA, Yakushevich LV (2015) Trajectories of DNA bubbles. *Chaos, Soliton Fract* 75: 62–75.
12. Yakushevich LV, Krasnobaeva LA (2019) Plasmid pBR322 and nonlinear conformational distortions (kinks). *Math Biol Bioinform* 14: 327–339.
13. Watson N (1988) A new revision of the sequence of plasmid pBR322. *Gene* 70: 399–403.
14. The pBR322 DNA sequence. Available from: http://www.ncbi.nlm.nih.gov/nuccore/J01749.1.
15. Krasnobaeva LA, Yakushevich LV (2015) Rotational dynamics of bases in the gene coding interferon alpha 17 (IFNA17). *J Bioinf Comput Biol* 13: 1540002.
16. Yakushevich LV, Krasnobaeva LA (2008) A new approach to studies of non-linear dynamics of kinks activated in inhomogeneous polynucleotide chains. *Int J Nonlin Mech* 43: 1074–1081.
17. Yakushevich L (2017) On the mechanical analogue of DNA. *J Biol Phys* 43: 113–125.
18. Yakushevich LV, Savin AV, Manevitch LI (2002) Nonlinear dynamics of topological solitons in DNA. *Phys Rev E* 66: 016614.
19. McLaughlin DW, Scott AC (1978) Perturbation analysis of fuxon dynamics. *Phys Rev A* 18: 1652–1658.
20. Yakushevich LV, Krasnobaeva LA (2007) Effects of dissipation and external fields on the dynamics of conformational distortions in DNA. *Biophysics* 52: 237–243.
21. Yakushevich LV, Ryasik AA (2012) Dynamical characteristics of DNA kinks and antikinks *Comput Res Model* 4: 209–217.

AIMS Press